Pioneer. Adv. Mater. 2026, 2(2): 1-18 DOI: 10.48308/piadm.2026.246813.1033

Pioneering Advances in Materials

Journal homepage: http://piadm.sbu.ac.ir ISSN: 3115-7114

Research paper

Advances and Challenges in DNA Sequencing Using Two-Dimensional Nanopores

Ahmed Al-Sheikh, Narges Nikoofard*

University of Kashan, Institute of Nanoscience and Nanotechnology

*nikoofard@kashanu.ac.ir

Article info:

Article history:

Received: 04/10/2026

Accepted: 24/11/2026

Keywords:

DNA sequencing; two-dimensional (2D) materials; graphene nanopores; MoS_2 nanopores; transverse electronic current

Abstract

Two-dimensional (2D) material nanopores offer great promise for single-molecule DNA sequencing. Their atomic thickness matches the spacing between adjacent nucleobases, providing high spatial resolution. This review summarizes recent progress in DNA sensing using graphene, molybdenum disulfide (MoS_2), hexagonal boron nitride (h-BN), tungsten disulfide (WS_2), and MXenes. Both ionic-current and transverse-electronic-current sensing mechanisms are considered, discussing key insights from experiments and molecular dynamics simulations. These studies clarify how pore geometry, surface chemistry, electric fields, and DNA conformations affect translocation signals. Graphene delivers atomic-scale resolution. However, strong hydrophobicity, membrane fluctuations, and high low-frequency noise often cause DNA sticking and pore clogging. In contrast, MoS_2 and h-BN feature lower DNA adhesion, greater stiffness, and higher signal-to-noise ratios. Transverse electronic current sensing provides wider measurement bandwidth and complementary base readout. Despite this progress, single-base resolution faces several key bottlenecks. These include rapid DNA translocation, high electrical noise, base conformational fluctuations, and low device yields. To solve these issues, researchers have developed various methods. These include ionic-liquid and viscosity gradients, surface-charge engineering, heterostructures, motion-control layers, hybrid field-effect transistor designs, and machine-learning analysis. Combining reliable materials synthesis, controlled DNA transport, and data-driven signal processing will be essential to realize practical, high-throughput 2D nanopore sequencing platforms.

Copyright: © 2025 by the authors. Submitted for possible open access publication under the terms and conditions of the Creative Commons Attribution (CC BY) license https://creativecommons.org/licenses/by/4.0/).

1. Introduction

Nanopores act as single-molecule sensing platforms for diverse biomolecules [1]. Nanopore-based DNA sequencing holds great promise as a low-cost, portable diagnostic technology [2]. In a typical setup (Figure 1a), voltage drives molecules through a pore, causing ionic current fluctuations that reveal analyte structure, length, and nucleobase sequence [3]. Biological nanopores pioneered this approach. Kasianowicz et al. first demonstrated single-stranded DNA/RNA translocation using α-hemolysin [4]. However, α-hemolysin's $\sim$ 5 nm sensing region spans about ten bases.

This yields an averaged signal that prevents single-base resolution [5].

In contrast, Mycobacterium smegmatis porin A (MspA) provides a shorter sensing zone ($\sim$ 0.5 nm), significantly improving base discrimination [6]. Solid-state nanopores (e.g., in SiN_x) offer superior mechanical/chemical stability and tunable geometry over biological pores [7].

However, conventional membranes ($\gtrsim$ 10 nm) remain too thick for base-level resolution. Consequently, two-dimensional (2D) materials have emerged as ideal alternatives. Solid-state and 2D material nanopores provide unprecedented physical robustness and integration potential for high-throughput single-molecule analysis [8].

Graphene features an atomic thickness ($\sim$ 0.34 nm) matches the inter-base spacing of DNA. It has excellent mechanical strength, and atom impermeability [9], successfully enabling DNA translocation sensing [10]. Other 2D materials such as h-BN [11] and MoS_2 [12] have also been developed. Furthermore, the electrical conductivity of graphene nanoribbons enables transverse electronic current sensing (Figure 1b), which can provide higher measurement bandwidth [13]. Despite these advancements, achieving high-resolution DNA sequencing with 2D nanopores remains obstructed by rapid DNA translocation and high ionic current noise [14]. Addressing these dual limitations requires a concerted synergy between optimizing ionic transport and implementing transverse electronic conductance modalities [15].

2. Detecting Ionic Current

In 2010, the Golovchenko [10], Dekker [17], and Drndić [18] groups first demonstrated double-stranded DNA (dsDNA) translocation through graphene nanopores (2–23 nm diameter, 1–15 layers) suspended over SiN_x apertures by monitoring transient current blockades.

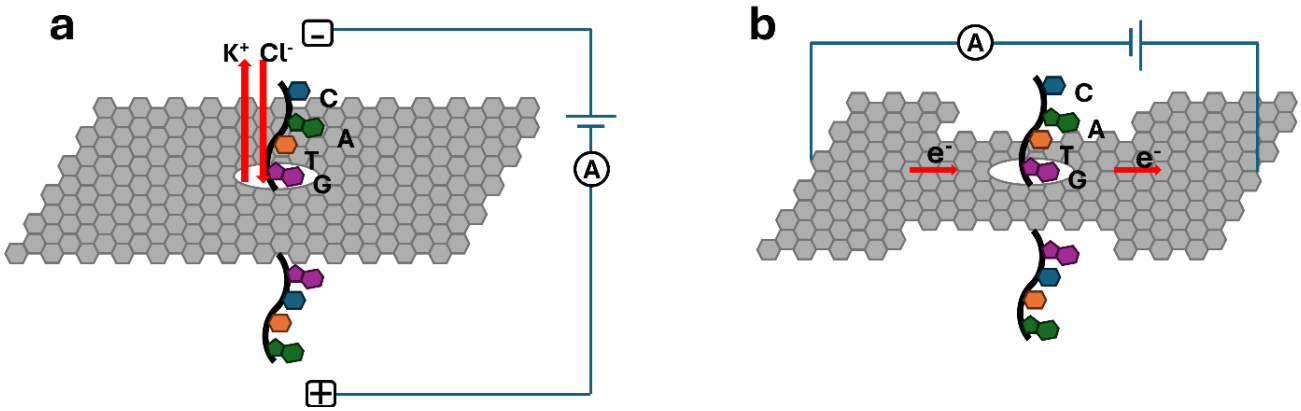


Figure 1. (a) Schematic illustration of a solid-state nanopore for ionic-current-based DNA sensing, where DNA translocation modulates the ionic current through the pore. (b) Conceptual schematic of DNA sequencing based on transverse electronic current, in which nucleotide-specific interactions influence the electronic signal across a nanogap (Idea from Ref. [16])

Besides, transition metal dichalcogenide nanopores have the capability to resolve distinct structural features of modified DNA conjugates via distinctive ionic blockade signatures [19].

The total resistance of a cylindrical nanopore includes pore resistance ($R_{\text{pore}} = \frac{4l}{\sigma\pi d^2}$) and access resistance ($2R_{\text{access}} = \frac{1}{\sigma d}$):

$$G = \frac{1}{R} = \sigma\left(\frac{4l}{\pi d^2} + \frac{1}{d}\right)^{-1}$$

where σ is ionic conductivity, d is diameter, and l is membrane thickness [20]. For monolayer graphene, access resistance dominates, yielding an $R \sim 1/d$ scaling [10] supported by simulations showing current density concentrated at pore edges [21].

In contrast, thicker membranes exhibit an $R \sim 1/d^2$ scaling [22].

An $R \sim 1/d^2$ scaling observed by Dekker et al. was attributed to surface coatings used to prevent DNA adhesion [17].

However, it should be noted that non-ideal pore geometry and atomic-scale edge irregularities play a dominant role in determining local translocation dynamics [23].

Recent progress in 2D nanopores focuses on reducing translocation speed and electrical noise while improving stability and fabrication reproducibility. High-viscosity systems and ionic liquids have been implemented to slow single-stranded DNA (ssDNA) translocation and improve signal-to-noise ratio in MoS_2 pores [24]. Additionally, edge surface-charge engineering in graphene nanopores reduces non-specific DNA adhesion and regulates translocation dynamics [25].

Experimentally, 2D nanopores have proven robust; for instance, MoS_2 devices exhibit stable open-pore conductance (G_{open}) over hours of continuous sensing (Figure 2) [26]. Furthermore, refined sequential fabrication methods have narrowed pore diameter distributions, significantly improving device reproducibility [27]. In addition, scalable bottom-up synthesis methods for nanoporous 2D membranes have emerged. They are a promising avenue to overcome conventional drilling variability and improve device yield [28].

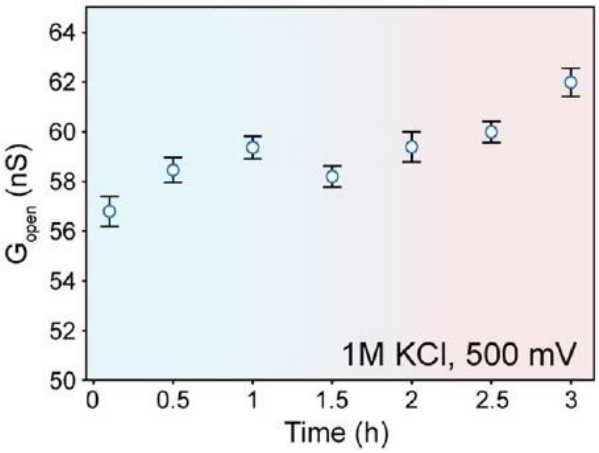


Figure 2. Time evolution of the mean open-pore conductance (G_{open}) of a two-dimensional MoS_2 nanopore during continuous DNA sensing. The minimal increase in conductance over more than 3 h at 1 M KCl and an applied bias of 500 mV indicates excellent long-term device stability and negligible performance degradation [26]

3. Simulations of Graphene Nanopores

All-atom molecular dynamics (MD) simulations have provided crucial atomistic insights into electric-field-driven DNA transport across graphene nanopores. Schulten's group demonstrated that the applied voltage drop is sharply localized across the ultrathin membrane [29].

This is similar to the localized potential drop in MspA biological pores and confirms graphene's potential for high spatial resolution [30].

Aksimentiev and co-workers showed that single-stranded DNA (ssDNA) exhibits strong hydrophobic affinity for graphene. This leads to adsorbtion, spreading, and undergoing lateral diffusion along the surface during translocation (Figure 3) [31]. Multilayer graphene (e.g., three layers) can facilitate stepwise single-nucleotide transport under low bias. Higher transmembrane

voltages often trigger skipping events where multiple nucleotides pass at once [31].

Furthermore, strong non-specific hydrophobic interactions frequently cause pore clogging and impede permeation. This underscores the need for surface functionalization or the exploration of alternative 2D nanomaterials [31, 32]. Recent studies indicate that sequence-dependent steric and electrostatic interactions exists in decorated MoS_2 nanopores.

These interactions can be exploited to achieve spontaneous translocation slowdown in atomically thin apertures [33].

4. Other 2D Materials as Graphene Substitutes

As was stated, graphene shows strong hydrophobic DNA adsorption (causing clogging and poor capture) and high out-of-plane membrane fluctuations. Thus, research has turned toward alternative 2D materials. Molybdenum disulfide (MoS_2) is thicker, stiffer, and less hydrophobic, yielding significantly reduced DNA adhesion. Translocation of unfolded, partially folded, and folded DNA through MoS_2 nanopores produces distinct ionic current blockade signatures (Figure 4) [12].

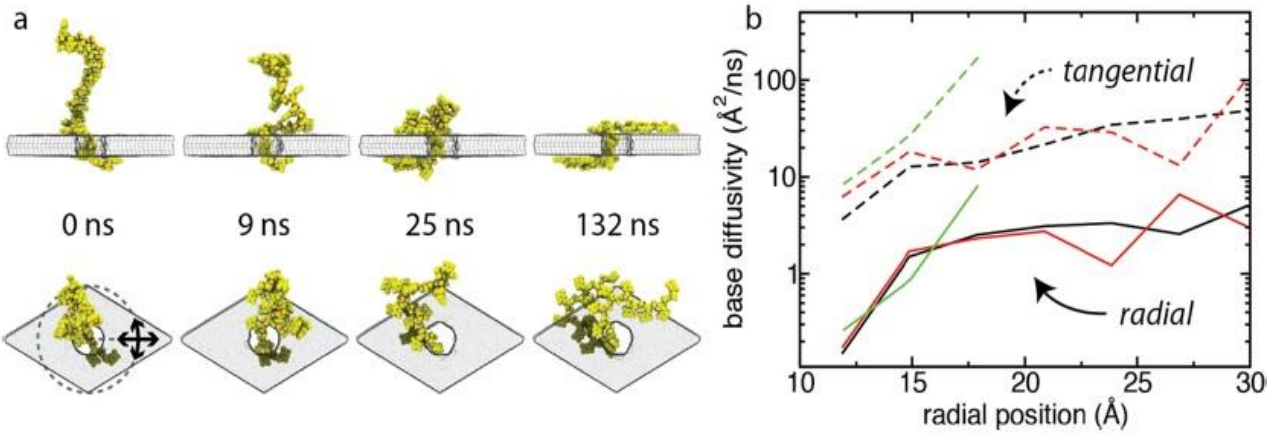


Figure 3. Adsorption and surface mobility of ssDNA on graphene. (a) Representative molecular dynamics snapshots illustrating the progressive adhesion and spreading of the ssDNA strand on the graphene membrane over time. (b) Base diffusivity as a function of radial position, demonstrating lateral motion of the adsorbed strand along the graphene surface in both radial and tangential directions [31]

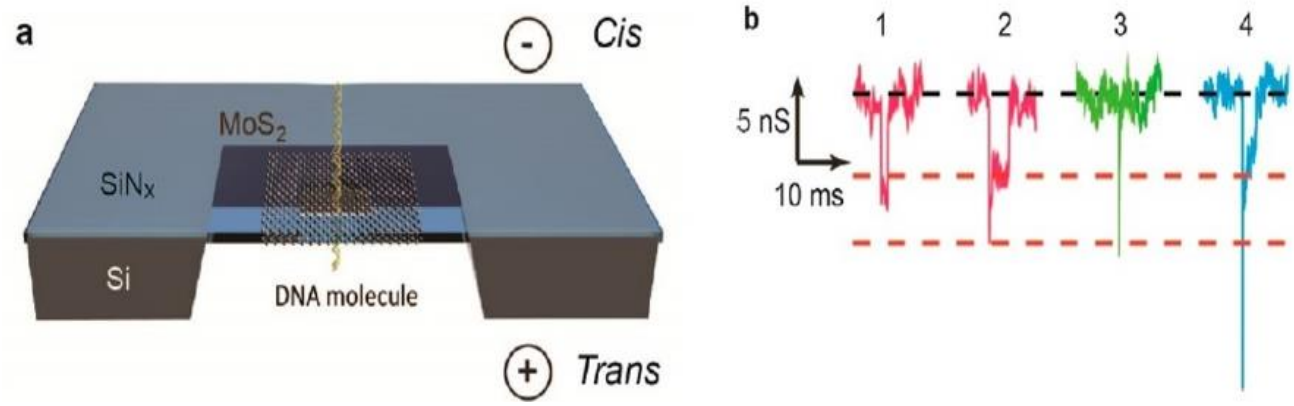


Figure 4. (a) Schematic illustration of electric-field-driven DNA translocation through a MoS_2nanopore. (b) Representative ionic current blockades corresponding to unfolded, partially folded, and fully folded λ-DNA translocation events through a 20 nm MoS_2 nanopore, demonstrating distinct signal signatures associated with different molecular conformations [12]

Experimentally, MoS_2 nanopores achieve high signal-to-noise ratios ($SNR > 10$) [12], while simulations show a superior SNR (15.02) compared to graphene (3.32) [34].

Furthermore, atomistic simulations of graphene–MoS_2 heterojunction pores are performed. They demonstrate that asymmetric local charge distributions can significantly enhance single-stranded DNA capture efficiency while modulating dwell times [35].

Comparative studies show that MoS_2 nanopores show reduced surface adhesion and distinct current fluctuation profiles. This facilitates continuous translocation with substantially diminished pore clogging [36].

Hexagonal boron nitride (h-BN) is an electrically insulating 2D analog of graphene that offers high chemical/electrical stability in salt solutions [11]. Importantly, h-BN supports the formation of atomically precise triangular nanopores (Figure 5) [37], with translocation mechanisms and blockade signatures confirmed experimentally and computationally [38]. Monolayer hexagonal boron nitride (h-BN) nanopores have demonstrated superior signal-to-noise ratios and baseline stability. This establishes h-BN as a prime candidate for robust solid-state biosensing [39]. Other 2D candidates, including WS_2 [40] and Mxenes [41], have also demonstrated viable DNA detection.

To present a direct comparison of the materials reviewed, Table 1 shows key physical, mechanical, and electronic parameters of the outstanding 2D membranes used in nanopore DNA sequencing. While graphene offers the best atomic thickness for single-nucleotide resolution, its hydrophobic $\pi - \pi$ interactions with DNA and high 1/f noise present severe fabrication and translocation challenges. In contrast, transition metal dichalcogenides such as MoS_2 and WS_2 provide excellent signal-to-noise ratios and reduced DNA sticking, while h-BN offers exceptional electrical insulation and atomic-precision pore shaping.

5. Transverse Electronic Current Detection

Transverse electronic current sensing in conductive 2D nanoribbons (e.g., graphene) offers an alternative sequencing modality. Base-specific electronic coupling locally modulates the ribbon's density of states (DOS) and transverse conductance during translocation [42]. DFT calculations indicate that semiconducting armchair nanoribbons can differentiate the four nucleobases largely independent of base orientation [42].

However, metallic zigzag ribbons provide higher (microampere-range) currents with orientation-dependent modulation [43].

Experimentally, Traversi et al. drilled a 10 nm pore in a ~ 100 nm-wide graphene ribbon. They demonstrated concurrent ionic current blockades and transverse current modulations via nonlocal capacitive coupling (Figure 6) [44, 16]. Similar field-effect detection was achieved using silicon nanowire [45] and pristine graphene nanoribbon FETs [13].

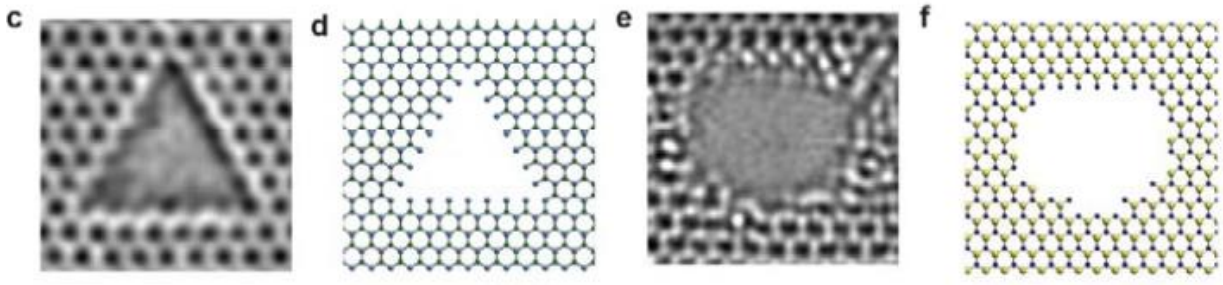


Figure 5. High-resolution transmission electron microscopy (HRTEM) image of a triangular nanopore in single-layer hexagonal boron nitride (h-BN), highlighting the well-defined and atomically precise pore geometry characteristic of this material [37]

Table 1. Summary of key physical, mechanical, electronic, and sensing properties of prominent two-dimensional (2D) materials investigated for nanopore DNA sequencing

2D Material	Typical Thickness (nm)	Mechanical Stability / Young's Modulus	DNA-Material Interaction / Adhesion	Electronic Nature & Conductivity	Signal-to-Noise Ratio (SNR) & Resolution	Key References
Graphene	~0.34 (Monolayer)	Ultrahigh in-plane stiffness; prone to rippling	Strong $\pi - \pi$ stacking; high hydrophobic adsorption	Semimetallic / Zero bandgap	Moderate; limited by high $1/f$ noise; single-nucleotide resolution	[12, 46]
MoS_2 (Molybdenum Disulfide)	~0.65 (Monolayer)	High stiffness and tear resistance	Lower hydrophobic adhesion than graphene; reduced DNA sticking	Semiconductor (Bandgap ~ 1.8 eV)	Superior to graphene due to lower dielectric noise; distinct blockade signatures	[34, 36, 48, 62]
h-BN (Hexagonal Boron Nitride)	~ 0.33 − 0.5	High mechanical strength and chemical inertness	Hydrophilic/neutral; minimal non-specific DNA adhesion	Wide-bandgap insulator (Bandgap~5.5 eV)	High baseline stability; supports atomically precise triangular pores	[28, 63]
WS_2 (Tungsten Disulfide)	~ 0.7	High mechanical robustness	Low non-specific adsorption similar to MoS_2	Semiconductor (Bandgap ~ 2.0 eV)	Good; compatible with light-adjustable pore sizes	[40]
MXenes($Ti_3C_2T_x$, etc.)	~1.0	Good in layered/flake form	Hydrophilic due to surface terminations (-OH ,-F)	Metallic / High electronic conductivity	Promising for transverse FET and electrochemical sensing	[41]

Later, scaling down to a ~ 30 nm ribbon with a 5 nm pore enabled direct detection of resistive (noncapacitive) modulations stemming from local DOS perturbations [46]. Vertical van der Waals heterojunctions are integrated with low-dimensional junction diodes directly across the nanopore.

They enable real-time electronic readout of translocating nucleobases with enhanced signal bandwidth [47].

Because graphene requires sub-10 nm patterning to open an adequate bandgap, naturally semiconducting MoS_2 has emerged as a compelling alternative. A ~ 2.5 nm pore in a 50 nm-wide MoS_2 ribbon enabled simultaneous ionic and transverse detection. In this setup, conductance shifts directly correlated with analyte charge (decreasing for DNA, remaining neutral for PEG, and increasing for polylysine) [48]. Recently, hybrid 2D Nanopore-FET platforms have enhanced bandwidth and reduced noise [49]. Besides, topological defect and edge engineering have improved electronic signal contrast among bases [50]. However, real-time single-base sequencing remains hindered by the need for atomic-scale structural precision.

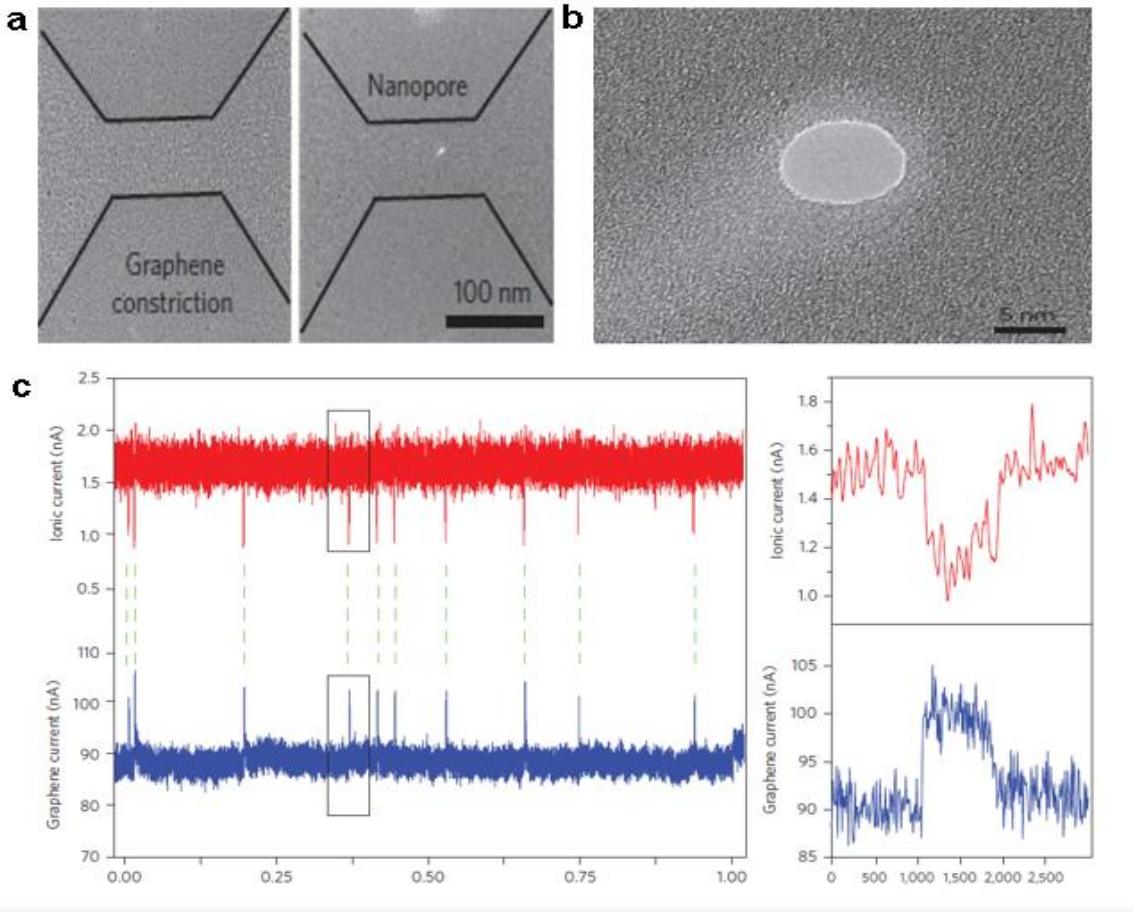


Figure 6. Fabrication and operation of a graphene nanoribbon nanopore device. (a) TEM images of the graphene nanoribbon constriction before and after nanopore drilling. (b) Magnified view of the nanopore formed at the center of the nanoribbon. (c) Correlated ionic current blockades and transverse graphene current modulations during DNA translocation, demonstrating simultaneous dual-signal detection [44]

5.1. Comparative Analysis: Ionic-Current vs. Transverse-Electronic-Current Detection

To date, two primary signal-transduction architectures have dominated two-dimensional (2D) solid-state nanopore sequencing: longitudinal ionic-current blockade detection and transverse electronic-current modulation. While both methods use the single-atom-thick profile of 2D membranes to achieve high spatial confinement, they differ fundamentally across several critical performance metrics, including sensitivity, temporal bandwidth, signal stability, fabrication yield, and scalable practical implementation.

Sensitivity and Signal-to-Noise Ratio (SNR)

Ionic-current sensing relies on measuring transient drops in electrophoretic ion flux through the pore volume during molecular passage. In atomically thin 2D membranes (e.g., monolayer graphene), the geometric pore resistance becomes comparable to or smaller than the access resistance [10, 22]. Consequently, small geometric or chemical variations at the pore perimeter dominate the effective ionic blockade, yielding moderate sensitivity that easily distinguishes folded vs. unfolded polynucleotide configurations [19] but struggles to reliably differentiate individual nucleobases without secondary deceleration or chemical functionalization.

In contrast, transverse electronic-current detection monitors direct electronic perturbations either

through quantum mechanical tunneling across nanogaps, local density-of-states (DOS) modulation across a semiconducting/metallic nanoribbon, or field-effect gating in a 2D nanopore-FET geometry [42–44]. Because this electronic coupling decays exponentially or abruptly with distance, it delivers exceptionally high local sensitivity capable of resolving individual nucleotide electronic fingerprints. However, this high sensitivity is acutely vulnerable to $1/f$ low-frequency noise, dielectric loss from the underlying substrate, and baseline fluctuations arising from molecular conformational dynamics inside the pore [46, 56].

Temporal Resolution and Bandwidth Limits

A major bottleneck in solid-state nanopore sequencing is the mismatch between analyte translocation velocity and the detection bandwidth. In standard ionic-current measurements, intrinsic translocation speeds of single-stranded DNA reach ~ 100 bp/μs under typical applied electric fields [59], whereas low-noise patch-clamp amplifiers operate typically at bandwidths below 100 kHz [7]. Consequently, ionic blockade events for single nucleotides are frequently missed or averaged out, demanding external deceleration strategies such as high-viscosity ionic liquids or engineered surface charges [24, 60].

Transverse electronic sensing enables intrinsic sub-microsecond response times and multi-megahertz operational bandwidths [47, 57]. The localized nature of the electronic readout in 2D nanoribbons provides the temporal resolution necessary to track single-base events in real time.

Baseline and Device Stability

Long-term signal stability is an important property of ionic-current platforms. In high-quality 2D nanopores, stable open-pore ionic conductances have been consistently demonstrated for operational durations exceeding several hours under physiological ionic strengths (e.g., 1.0 M KCl) with negligible baseline drift [26].

Conversely, transverse electronic devices are inherently prone to baseline instabilities. Electrochemical gating by the charge-trapping phenomena within adjacent supporting oxide layers and degradation of 2D/metal electrical contacts during continuous fluidic exposure often induce severe threshold voltage drifts and device failure, requiring sophisticated surface passivation layers (e.g., atomic layer deposition of Al_2O_3 or HfO_2) [49].

Fabrication Complexity and Practical Scalability

The most important difference between the two methods lies in manufacturing yield and device integration. Ionic-current systems require only the fabrication of an isolated sub-nanometer pore within a suspended 2D membrane positioned over a supporting silicon nitride (SiN_x) aperture. While transmission electron microscopy (TEM) drilling remains low-throughput, scalable chemical and controlled dielectric breakdown (CBD) methods have significantly improved process reproducibility [72–74].

By comparison, transverse electronic sensing requires lithographic patterning and precise sub-nanometer alignment of a nanopore within an ultra-narrow (sub-50 nm) conductive nanoribbon or between nanoelectrodes [44, 46]. It is prone to membrane tearing, mechanical strain, interfacial contamination, and nanoribbon cracking result in high rates.

Reported functional device yields are extraordinarily low typically on the order of ~ 1 functional device out of 180 in graphene nanoribbons [46] and ~ 3 out of 200 in MoS_2 platforms [48].

Hence, while transverse electronic readout offers superior theoretical resolution and array integration capabilities, ionic-current detection remains the more practically mature and reliable method for immediate sequencing applications.

A quantitative and comparative summary of both sensing strategies is presented in Table 2.

Table 2. Comparative evaluation of ionic-current and transverse electronic-current sensing modalities for 2D nanopore DNA sequencing

Performance Metric	Ionic-Current Sensing	Transverse Electronic-Current Sensing	Key References
Sensing Mechanism	Transient blockade of electrophoretic ionic current through the pore orifice	Local density of states (DOS) modulation, quantum tunneling, or field-effect conductance shifts	[10, 17, 42, 44]
Spatial / Base Resolution	Moderate; detects conformational state and nucleotide clusters; single-base resolution requires severe deceleration	Very high; atomic-scale localized electronic coupling permits intrinsic single-nucleotide distinction	[12, 19, 43, 46]
Temporal Resolution & Bandwidth	Limited (∼10–100 kHz) by amplifier capacitance and fast molecular translocation (∼100 bp/μs)	High (sub-microsecond response, >1 MHz bandwidth); less constrained by translocation speed	[7, 47, 57, 59]
Signal-to-Noise Ratio (SNR)	Moderate to high (material-dependent; MoS_2 and h-BN outperform graphene); dominated by access resistance	Highly variable; limited by severe $1/f$ flicker noise, gate leakage, and capacitive substrate coupling	[58, 56, 48]
Signal Stability & Longevity	High; exhibits stable baseline open-pore conductance over hours with minimal drift	Moderate to low; prone to contact degradation, electrochemical charge traps, and threshold drift	[26, 46, 49]
Fabrication Complexity	Low to moderate; requires a single nanopore drilled into a suspended 2D membrane	Extremely high; necessitates sub-nanometer lithographic alignment of nanoribbons/electrodes across the pore	[44, 46, 72]
Device Yield	Relatively moderate to high via scalable techniques (e.g., controlled breakdown)	Extremely low (∼0.5%–1.5% yield in functional nanoribbon/FET configurations)	[46, 73, 74]
Practical Scalability	Well-established for fluidic parallelization; commercial precedent in biological/solid-state platforms	Promising for CMOS-integrated semiconductor architectures, but hampered by manufacturing yield	[45, 47, 49, 75]

6. Challenges in DNA Sequencing Using 2D Nanopores

Despite extensive progress, neither ionic nor transverse current modalities in 2D material nanopores have achieved reliable single-nucleobase resolution or a complete experimental proof-of-concept for sequencing. This limitation stems from several interrelated bottlenecks.

First, high stochastic fluctuations degrade both ionic and transverse readout, obscuring nucleotide-specific current signatures [24]. Besides, strong hydrophobic interactions particularly on graphene cause erratic ssDNA accumulation and signal variability. This can be mitigated via chemical or surface-charge functionalization [25]. Variations in pore dimensions hinder repeatability, though advanced methods (e.g., cascaded fabrication) have narrowed diameter distributions [27]. Finally, rapid passage prevents sufficient dwell time for base discrimination. This requires active velocity regulation and advanced materials engineering. Overcoming these obstacles will require integrated solutions combining material optimization, nanoscale device engineering, and advanced signal processing.

6.1. Noise Reduction in Nanopore Measurements

The signal-to-noise ratio (SNR) in 2D material nanopores is severely constrained by elevated electrical noise compared to thicker solid-state membranes (e.g., SiN_x) [51]. Low-frequency $1/f$ noise (< 1 kHz) is attributed to mechanical out-of-plane fluctuations, poor surface wetting, nanobubbles [52], and structural defects [16]. To mitigate this, several mechanical stabilization strategies have been implemented. Using few-layer membranes suppresses $1/f$ noise by ~ 1.5 orders of magnitude [51]. However, excessive thickening compromises spatial resolution. Protective oxide coatings (e.g., ~ 5 nm TiO_2 [18] or graphene/Al_2O_3 heterostructures [53]) also have the same effect.

Restricting the membrane area exposed to electrolyte lowers mechanical fluctuations in both graphene and multilayer h-BN. Thus, the fluctuations match SiN_x baseline noise levels [54]. Besides, direct, transfer-free growth on supporting apertures eliminates transfer-induced defects and grain-boundary noise [55]. At higher frequencies (> 1 kHz), capacitance-dependent dielectric noise dominates [56, 57]. Implementing high-quality dielectric supporting substrates reduces effective capacitance and improves high-bandwidth fidelity [58]. Additionally, transverse electronic current sensing in MoS_2 demonstrated a $\sim 40\%$ higher SNR than simultaneous ionic current detection [48]. This underscores the promise of transverse modalities for overcoming high-bandwidth noise bottlenecks.

6.2. Control of DNA Translocation Speed

Excessively rapid translocation constitutes a primary bottleneck in solid-state nanopore sequencing. Resolving single bases requires velocities around 1–100 bp/ms to match typical amplifier bandwidths [7]. However, intrinsic translocation speeds in 2D material nanopores reach 2×10^4–1×10^5 bp/ms [59]. To bridge this gap without compromising the atomic-scale spatial resolution of 2D membranes, several deceleration paradigms have been developed.

Exploiting strong hydrophobic graphene–DNA interactions in graphene/Al_2O_3/graphene sandwiches significantly retards DNA passage [60]. Similarly, graphene/MoS_2 heteropores induce asymmetric, direction-dependent translocation speeds [61]. Besides, implementing an asymmetric ionic liquid/KCl interface across an MoS_2 nanopore slowed translocation to ~ 373 bp/ms (a ~ 100-fold reduction). This approach enabled ionic-current discrimination of

all four DNA homopolymers and single nucleotides [62]. Viscosity-tuned ionic liquid mixtures show similar deceleration in h-BN pores [63].

In one method, the surface charge density of graphene is modulated between negative (arrest/repulsion) and positive (acceleration). The method enables enzyme-free, stepwise "stop-and-go" ratchet motion of ssDNA (Figures 7 and 8) [64]. In MoS_2 nanopores, tuning edge Mo:S stoichiometry alters the balance between electrophoretic and electroosmotic forces. This approach is capable of decelerating or even reversing translocation [65]. For transverse electronic current sensing, intrinsic high bandwidths alleviate strict velocity limits. Coupling moderate slowdown strategies (e.g., viscosity gradients) with high-speed nanoribbon readouts presents a viable route to robust single-base discrimination.

6.3. Preventing DNA Fluctuations in Nanopores

Positional, orientational, and conformational fluctuations of nucleobases within nanopores degrade the SNR by broadening conductance distributions. This is a bottleneck especially severe for transverse electronic sensing, where electronic coupling depends exponentially on nucleotide orientation [66, 67]. While early idealized DFT models with static, isolated nucleotides predicted distinct base signatures [66], realistic MD simulations incorporating thermal noise, ions, and solvent reveal substantial signal overlap [67].

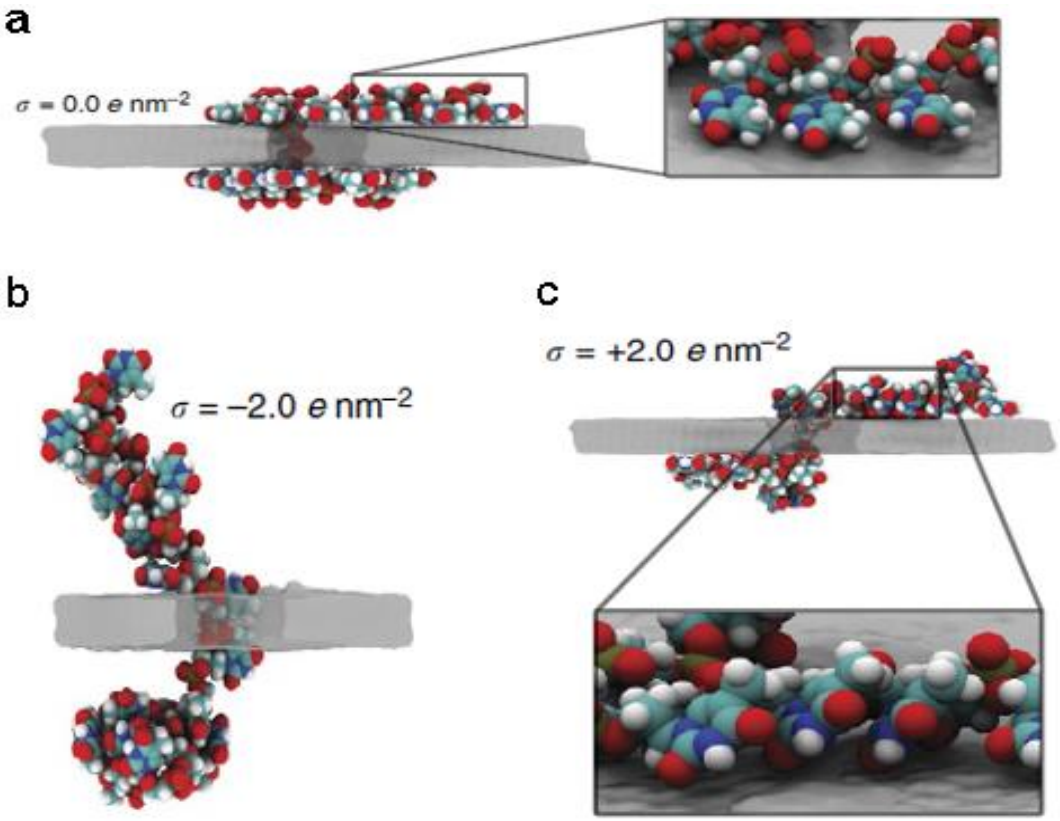


Figure 7. Effect of graphene surface charge density on the conformation of translocating single-stranded DNA (ssDNA). Representative molecular dynamics snapshots illustrate distinct ssDNA configurations under (a) neutral, (b) negative, and (c) positive graphene surface charge densities, highlighting the strong influence of electrostatic interactions on DNA adsorption and structural dynamics near the nanopore [64]

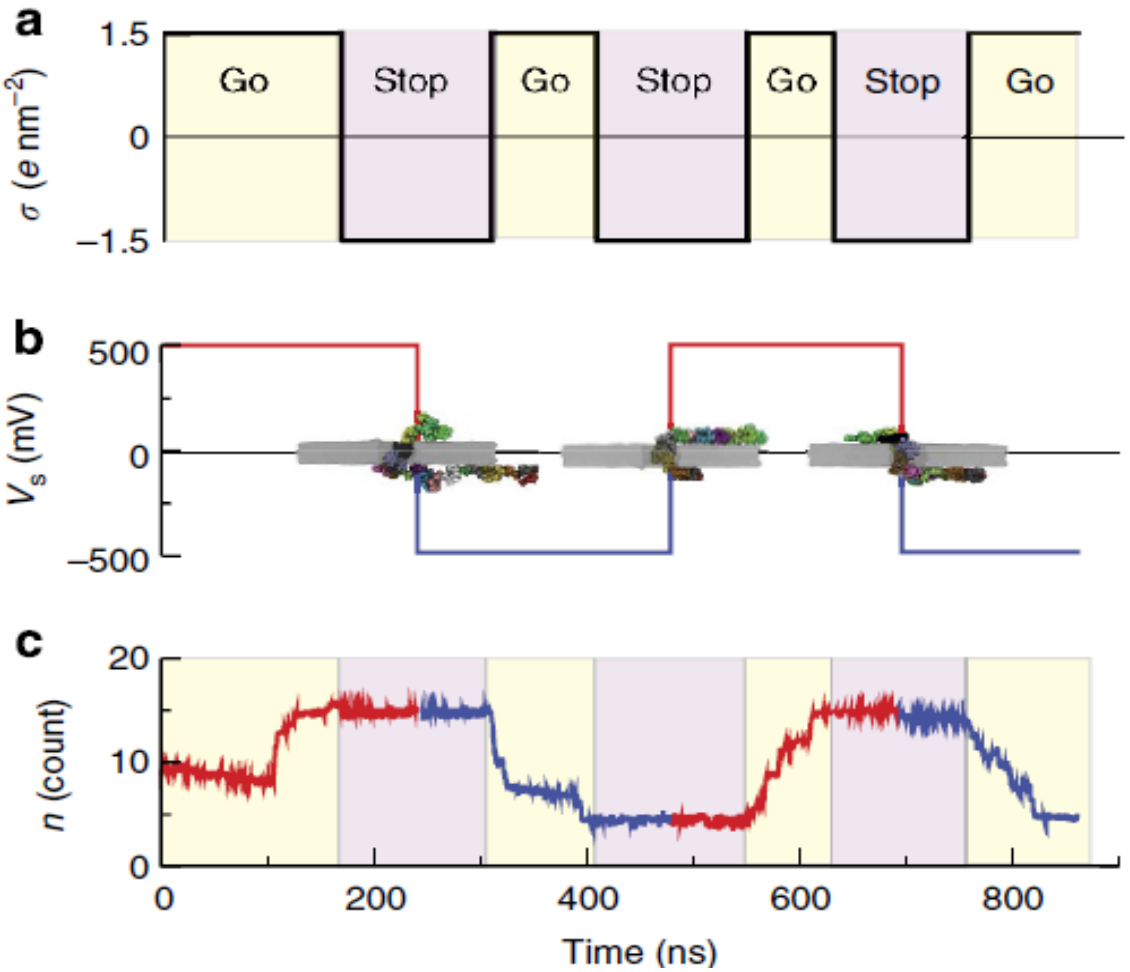


Figure 8. Charge-controlled stop-and-go transport of ssDNA through a graphene nanopore. (a) Time-dependent modulation of graphene surface charge density. (b) Applied transmembrane bias during the simulation. (c) Number of nucleotides translocated to the trans side as a function of time, demonstrating that positive surface charge promotes DNA transport, whereas negative charge effectively suppresses or arrests translocation, enabling controllable stepwise motion [64]

To suppress these fluctuations and constrain DNA motion within the sensing zone, several structural and electrostatic strategies have been introduced. Mechanically stretching ssDNA extends it in a ribbon-like conformation via hydrophobic graphene adhesion.

This suppresses out-of-plane nucleobase fluctuations and induces stepwise translocation, enabling single-base transverse resolution (Figure 9) [68]. Experimentally, such stretching occurs when electric fields thread ssDNA through tailored pore diameters [69]. Embedding an auxiliary metallic control layer beneath the sensing membrane generates an electrostatic attraction upon positive biasing. This locks the DNA against the pore wall and mitigates thermal vibrations (Figure 10) [70].

Dual-pore designs integrating a monolayer MoS_2 sensing pore above a guiding support spatially also confine DNA motion [71]. Besides, targeted edge functionalization stabilizes translocating nucleobases.

6.4. Practical and Fabrication Challenges

Several barriers still limit the practical development of 2D-material nanopores for DNA sequencing. Fabrication yield is extremely low. Only 1 of approximately 180 graphene nanoribbon devices remained functional after integration [46].

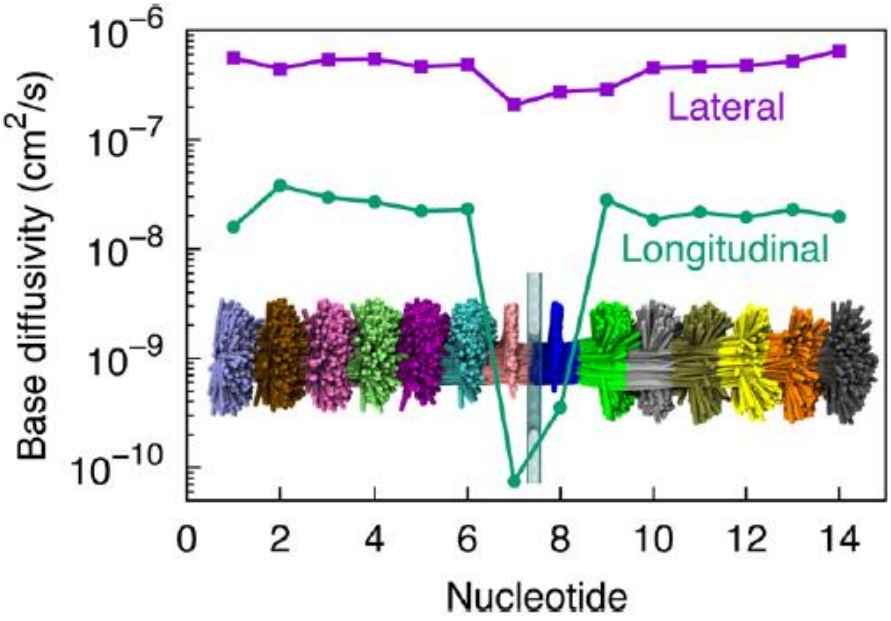


Figure 9. Suppression of nucleobase fluctuations in stretched single-stranded DNA (ssDNA) translocating through a graphene nanopore. Analysis of lateral and longitudinal diffusivities demonstrates that strong adhesion between ssDNA and the graphene surface significantly reduces out-of-plane fluctuations, thereby stabilizing nucleobase positions relative to the membrane and enhancing conditions for high-resolution sensing [68]

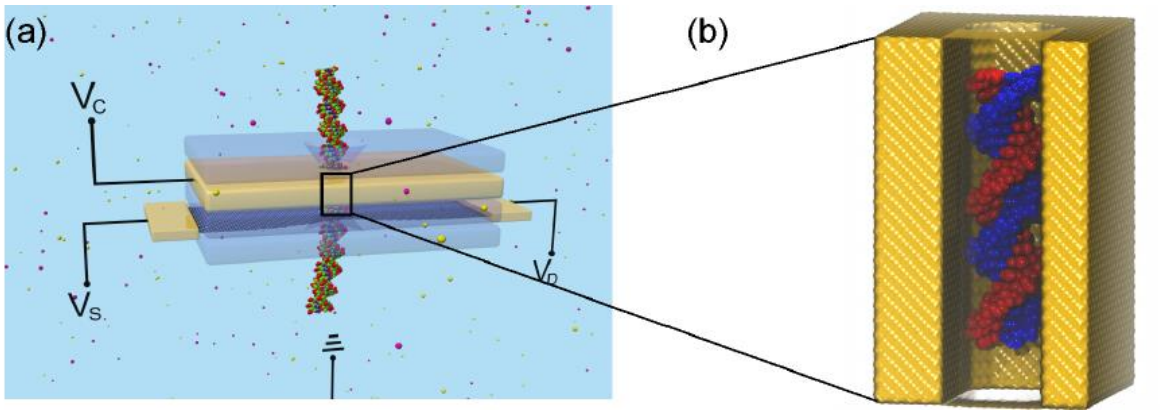


Figure 10. Multilayer nanopore architecture with an integrated motion-control layer for DNA stabilization. (a) Schematic illustration of a stacked membrane device comprising a metallic control layer embedded between insulating layers and a sensing membrane for DNA detection. Positive bias applied to the control layer modifies the local electrostatic environment within the nanopore and enhances DNA–surface attraction. (b) Molecular dynamics simulation of DNA confined within the nanopore of the biased multilayer membrane, illustrating suppression of thermal fluctuations and stabilization of DNA under an applied control voltage [70]

Besides, just 3 of about 200 MoS_2 devices detected DNA translocation [48]. Failures commonly arise from SiN_x membrane rupture, nanoribbon cracking, and contamination near the pore. Reproducible pore fabrication is another challenge. Indeed, the precise control of pore size and geometry is difficult. h-BN may offer an advantage through its well-defined triangular pores [37]. Although TEM enables nanometer-scale fabrication, it is costly, slow, and difficult to scale [72].

Electrical breakdown and electrochemical methods provide TEM-free alternatives for fabricating graphene [73] and MoS_2 [74] nanopores may help overcome the limitations of TEM. Finally, wafer-scale growth, transfer, and

integration may help overcome the limitations of small-area 2D-film processing [75].

7. Summary and Outlook

Atomically thin 2D materials (graphene, MoS_2, and h-BN) offer single-nucleotide spatial resolution for nanopore sequencing. However, ionic current sensing remains constrained by high $1/f$ noise. Besides, translocation speeds exceed measurement bandwidths. Transverse electronic sensing (e.g., via nanoribbons or nanopore-FETs) provides higher bandwidth and array scalability. It alleviates strict velocity limits, but suffers from low fabrication yields, sub-10 nm lithography challenges, and nucleobase conformational fluctuations. Each material presents trade-offs. Atomic thinness of graphene enables maximal resolution. However, its gapless band structure requires sub-10 nm ribbon patterning for transverse sensing. Tri-layer configurations offer better noise suppression and stepwise motion than monolayers [31]. h-BN provides precise triangular pore geometries, though its insulating nature limits transverse readout [76]. MoS_2 offers superior SNR, mechanical robustness, and lower DNA adhesion. MoS_2 successfully resolves nucleotides under viscosity gradients [62]. Beyond DNA sequencing, 2D nanopores are expanding toward DNA methylation mapping [77] and protein sequencing [78]. However, distinguishing all 20 amino acids remains challenging due to signal overlap [78]. Addressing these bottlenecks requires machine learning methods (convolutional neural networks or CNNs, and support vector machines or SVMs). These methods are used for noise-resilient base classification [79, 80], deploying multimodal sensing (simultaneous ionic and transverse readouts) [49], and exploring emerging materials like MXenes and heterostructures [81]. Ultimately, converging scalable material synthesis, motion-control architectures, and data-driven signal processing is essential to transition 2D nanopores from proof-of-concept devices to high-throughput sequencing platforms.

References

[1] D. Branton *et al.*, “The potential and challenges of nanopore sequencing,” *Nat. Biotechnol.*, vol. 26, no. 10, pp. 1146–1153, 2008.

[2] J. Shendure and H. Ji, “Next-generation DNA sequencing,” *Nat. Biotechnol.*, vol. 26, no. 10, pp. 1135–1145, 2008.

[3] E. A. Manrao *et al.*, “Reading DNA at single-nucleotide resolution with a mutant MspA nanopore and phi29 DNA polymerase,” *Nat. Biotechnol.*, vol. 30, no. 4, pp. 349–353, 2012.

[4] J. J. Kasianowicz, E. Brandin, D. Branton, and D. W. Deamer, “Characterization of individual polynucleotide molecules using a membrane channel,” *Proc. Natl. Acad. Sci.*, vol. 93, no. 24, pp. 13770–13773, 1996.

[5] D. Stoddart, A. J. Heron, E. Mikhailova, G. Maglia, and H. Bayley, “Single-nucleotide discrimination in immobilized DNA oligonucleotides with a biological nanopore,” *Proc. Natl. Acad. Sci.*, vol. 106, no. 19, pp. 7702–7707, 2009.

[6] M. Faller, M. Niederweis, and G. E. Schulz, “The structure of a mycobacterial outer-membrane channel,” *Science*, vol. 303, no. 5661, pp. 1189–1192, 2004.

[7] B. M. Venkatesan and R. Bashir, “Solid-state nanopore sensors for nucleic acid analysis,” *Nanopores Sens. Fundam. Biol. Interact.*, pp. 1–33, 2011.

[8] X.-L. Xing et al., “Nanopores in 2D materials and their applications in single molecule analysis,” *Trends Analyt. Chem.*, vol. 179, p. 117863, 2024.

[9] K. S. Novoselov *et al.*, "Electric field effect in atomically thin carbon films," S*cience*, vol. 306, no. 5696, pp. 666–669, 2004.

[10] S. Garaj, W. Hubbard, A. Reina, J. Kong, D. Branton, and J. Golovchenko, "Graphene as a subnanometre trans-electrode membrane," *Nature*, vol. 467, no. 7312, pp. 190–193, 2010.

[11] S. Liu *et al.*, "Boron nitride nanopores: highly sensitive DNA single-molecule detectors.," *Adv. Mater. Deerfield Beach Fla*, vol. 25, no. 33, pp. 4549–4554, 2013.

[12] K. Liu, J. Feng, A. Kis, and A. Radenovic, "Atomically thin molybdenum disulfide nanopores with high sensitivity for DNA translocation," *ACS Nano*, vol. 8, no. 3, pp. 2504–2511, 2014.

[13] M. Puster *et al.*, "Cross-Talk Between Ionic and Nanoribbon Current Signals in Graphene Nanoribbon-Nanopore Sensors for Single-Molecule Detection," *Small*, vol. 11, no. 47, pp. 6309–6316, 2015.

[14] C. Dekker, "Solid-state nanopores," *Nat. Nanotechnol.*, vol. 2, no. 4, pp. 209–215, 2007.

[15] R. L. Kumawat, M. K. Jena, S. Mittal, and B. Pathak, "Advancement of Next-Generation DNA Sequencing through Ionic Blockade and Transverse Tunneling Current Methods," *Small*, vol. 20, no. 38, p. 2401112, 2024.

[16] S. J. Heerema and C. Dekker, "Graphene nanodevices for DNA sequencing," *Nat. Nanotechnol.*, vol. 11, no. 2, pp. 127–136, 2016.

[17] G. F. Schneider *et al.*, "DNA translocation through graphene nanopores," *Nano Lett.*, vol. 10, no. 8, pp. 3163–3167, 2010.

[18] C. A. Merchant *et al.*, "DNA translocation through graphene nanopores," *Nano Lett.*, vol. 10, no. 8, pp. 2915–2921, 2010.

[19] J. Abourahma, T. Udumulla, R. Sha, J. W. Canary, and A. Sinitskii, "Synthesis of Nanographene-DNA Conjugates and Their Profiling with MoS_2 Nanopores," *Nano Lett.*, vol. 25, no. 15, pp. 6101–6108, 2025.

[20] M. Wanunu, T. Dadosh, V. Ray, J. Jin, L. McReynolds, and M. Drndić, "Rapid electronic detection of probe-specific microRNAs using thin nanopore sensors," *Nat. Nanotechnol.*, vol. 5, no. 11, pp. 807–814, 2010.

[21] S. Garaj, S. Liu, J. A. Golovchenko, and D. Branton, "Molecule-hugging graphene nanopores," *Proc. Natl. Acad. Sci.*, vol. 110, no. 30, pp. 12192–12196, 2013.

[22] J. E. Hall, "Access resistance of a small circular pore.," *J. Gen. Physiol.*, vol. 66, no. 4, pp. 531–532, 1975.

[23] Q. Sun et al., "Graphene Nanopore Fabrication and Applications," *Int. J. Mol. Sci.*, vol. 26, no. 4, p. 1709, 2025.

[24] Z. Gu, Z. He, F. Chen, L. Meng, J. Feng, and R. Zhou, "Ionic liquid decelerates single-stranded DNA transport through molybdenum disulfide nanopores," *ACS Appl. Mater. Interfaces*, vol. 14, no. 28, pp. 32618–32624, 2022.

[25] Y.-S. Zhang, Z.-Y. Qi, M.-M. Ding, M.-L. Li, and T.-F. Shi, "Translocation of ssDNA through charged graphene nanopores: effect of the charge density," *Chin. J. Polym. Sci.*, vol. 42, no. 12, pp. 2048–2058, 2024.

[26] M. Thakur *et al.*, "High durability and stability of 2D nanofluidic devices for long-term single-molecule sensing," *Npj 2D Mater. Appl.*, vol. 7, no. 1, p. 11, 2023.

[27] J. Wang *et al.*, "Cascaded compression of size distribution of nanopores in monolayer graphene," *Nature*, vol. 623, no. 7989, pp. 956–963, 2023.

[28] A. E. Naclerio et al., "Scalable Bottom-Up Synthesis of Nanoporous Hexagonal Boron Nitride (h-BN) for Large-Area Atomically Thin Ceramic Membranes," *Nano Lett.*, vol. 25, no. 8, pp. 3221–3232, 2025.

[29] C. Sathe, X. Zou, J.-P. Leburton, and K. Schulten, "Computational investigation of DNA detection using graphene nanopores," *ACS Nano*, vol. 5, no. 11, pp. 8842–8851, 2011.

[30] W. Zhou, H. Qiu, Y. Guo, and W. Guo, "Molecular insights into distinct detection properties of α-hemolysin, MspA, CsgG, and aerolysin nanopore sensors," *J. Phys. Chem. B*, vol. 124, no. 9, pp. 1611–1618, 2020.

[31] D. B. Wells, M. Belkin, J. Comer, and A. Aksimentiev, "Assessing graphene nanopores for sequencing DNA," *Nano Lett.*, vol. 12, no. 8, pp. 4117–4123, 2012.

[32] G. F. Schneider *et al.*, "Tailoring the hydrophobicity of graphene for its use as nanopores for DNA translocation," *Nat. Commun.*, vol. 4, no. 1, p. 2619, 2013.

[33] D. Zhang, M. Zhang, and R. Zhou, "Sequence-Dependent Slowdown of DNA Translocation Using Transmembrane RNA–DNA Interactions in MoS_2 Nanopore," *J. Phys. Chem. B*, vol. 129, no. 3, pp. 876–885, 2025.

[34] A. B. Farimani, K. Min, and N. R. Aluru, "DNA base detection using a single-layer MoS2," *ACS Nano*, vol. 8, no. 8, pp. 7914–7922, 2014.

[35] Y. Zhang and M. Ding, "Graphene-MoS_2 Heterojunction Nanopores: Enhanced ssDNA Capture via Asymmetric Charge Control," *J. Phys. Chem. B*, vol. 129, no. 49, pp. 12790–12797, 2025.

[36] P. Wei, M. Kansari, and M. Fyta, "Graphene or MoS_2 nanopores: pore adhesion and protein linearization," *Nanoscale*, vol. 17, no. 7, pp. 3873–3883, 2025.

[37] K. Liu *et al.*, "Geometrical effect in 2D nanopores," *Nano Lett.*, vol. 17, no. 7, pp. 4223–4230, 2017.

[38] Z. Gu, Y. Zhang, B. Luan, and R. Zhou, "DNA translocation through single-layer boron nitride nanopores," *Soft Matter*, vol. 12, no. 3, pp. 817–823, 2016

[39] T.-R. Liu et al., "Single-Layer Hexagonal Boron Nitride Nanopores as High-Performance Ionic Gradient Power Generators," *Small*, vol. 20, no. 16, p. 2306018, 2024.

[40] G. Danda *et al.*, "Monolayer WS_2 nanopores for DNA translocation with light-adjustable sizes," *ACS Nano*, vol. 11, no. 2, pp. 1937–1945, 2017.

[41] M. Mojtabavi, A. VahidMohammadi, W. Liang, M. Beidaghi, and M. Wanunu, "Single-molecule sensing using nanopores in two-dimensional transition metal carbide (MXene) membranes," *ACS Nano*, vol. 13, no. 3, pp. 3042–3053, 2019.

[42] T. Nelson, B. Zhang, and O. V. Prezhdo, "Detection of nucleic acids with graphene nanopores: ab initio characterization of a novel sequencing device," *Nano Lett.*, vol. 10, no. 9, pp. 3237–3242, 2010.

[43] K. K. Saha, M. Drndic, and B. K. Nikolic, "DNA base-specific modulation of microampere transverse edge currents through a metallic graphene nanoribbon with a nanopore," *Nano Lett.*, vol. 12, no. 1, pp. 50–55, 2012.

[44] F. Traversi *et al.*, "Detecting the translocation of DNA through a nanopore using graphene nanoribbons," *Nat. Nanotechnol.*, vol. 8, no. 12, pp. 939–945, 2013.

[45] P. Xie, Q. Xiong, Y. Fang, Q. Qing, and C. M. Lieber, "Local electrical potential detection of DNA by nanowire–nanopore sensors," *Nat.*

Nanotechnol., vol. 7, no. 2, pp. 119–125, 2012.

[46] S. J. Heerema, L. Vicarelli, S. Pud, R. N. Schouten, H. W. Zandbergen, and C. Dekker, "Probing DNA translocations with inplane current signals in a graphene nanoribbon with a nanopore," *ACS Nano*, vol. 12, no. 3, pp. 2623–2633, 2018.

[47] S. Chen et al., "Detecting DNA translocation through a nanopore using a van der Waals heterojunction diode," *Proc. Natl. Acad. Sci. U.S.A.*, vol. 122, no. 18, p. e2422135122, 2025.

[48] M. Graf, M. Lihter, D. Altus, S. Marion, and A. Radenovic, "Transverse detection of DNA using a MoS_2 nanopore," *Nano Lett.*, vol. 19, no. 12, pp. 9075–9083, 2019.

[49] J. Wei, H. Hong, X. Wang, X. Lei, M. Ye, and Z. Liu, "Nanopore-based sensors for DNA sequencing: a review," *Nanoscale*, vol. 16, no. 40, pp. 18732–18766, 2024.

[50] R. L. Kumawat and B. Pathak, "Extended topological line defects in graphene for individual identification of DNA nucleobases," *Mater. Adv.*, vol. 1, no. 8, pp. 2908–2916, 2020.

[51] S. Heerema, G. Schneider, M. Rozemuller, L. Vicarelli, H. Zandbergen, and C. Dekker, "1/f noise in graphene nanopores," *Nanotechnology*, vol. 26, no. 7, p. 074001, 2015.

[52] R. M. Smeets, U. Keyser, M. Wu, N. Dekker, and C. Dekker, "Nanobubbles in solid-state nanopores," *Phys. Rev. Lett.*, vol. 97, no. 8, p. 088101, 2006.

[53] B. M. Venkatesan *et al.*, "Stacked graphene-Al_2O_3 nanopore sensors for sensitive detection of DNA and DNA–protein complexes," *ACS Nano*, vol. 6, no. 1, pp. 441–450, 2012.

[54] K.-B. Park *et al.*, "Noise and sensitivity characteristics of solid-state nanopores with a boron nitride 2-D membrane on a pyrex substrate," *Nanoscale*, vol. 8, no. 10, pp. 5755–5763, 2016.

[55] P. Waduge, J. Larkin, M. Upmanyu, S. Kar, and M. Wanunu, "Programmed synthesis of freestanding graphene nanomembrane arrays," *Biophys. J.*, vol. 108, no. 2, p. 330a, 2015.

[56] K. Lee *et al.*, "Recent progress in solid-state nanopores," *Adv. Mater.*, vol. 30, no. 42, p. 1704680, 2018.

[57] J. K. Rosenstein, M. Wanunu, C. A. Merchant, M. Drndic, and K. L. Shepard, "Integrated nanopore sensing platform with sub-microsecond temporal resolution," *Nat. Methods*, vol. 9, no. 5, pp. 487–492, 2012.

[58] A. Kumar, K.-B. Park, H.-M. Kim, and K.-B. Kim, "Noise and its reduction in graphene based nanopore devices," *Nanotechnology*, vol. 24, no. 49, p. 495503, 2013.

[59] H. Arjmandi-Tash, L. A. Belyaeva, and G. F. Schneider, "Single molecule detection with graphene and other two-dimensional materials: nanopores and beyond," *Chem. Soc. Rev.*, vol. 45, no. 3, pp. 476–493, 2016.

[60] S. Banerjee *et al.*, "Slowing DNA transport using graphene–DNA interactions," *Adv. Funct. Mater.*, vol. 25, no. 6, pp. 936–946, 2015.

[61] B. Luan and R. Zhou, "Spontaneous transport of single-stranded DNA through graphene–MoS_2 heterostructure nanopores," *ACS Nano*, vol. 12, no. 4, pp. 3886–3891, 2018.

[62] J. Feng *et al.*, "Identification of single nucleotides in MoS_2 nanopores," *Nat. Nanotechnol.*, vol. 10, no. 12, pp. 1070–1076, 2015.

[63] J. S. Lee *et al.*, "Detection of nucleotides in hydrated ssDNA via 2D h-BN nanopore with ionic-liquid/salt–water interface," *Electrophoresis*, vol. 42, no. 7–8, pp. 991–

1002, 2021.

[64] M. Shankla and A. Aksimentiev, "Conformational transitions and stop-and-go nanopore transport of single-stranded DNA on charged graphene," *Nat. Commun.*, vol. 5, no. 1, p. 5171, 2014.

[65] W. Si, Y. Zhang, J. Sha, and Y. Chen, "Controllable and reversible DNA translocation through a single-layer molybdenum disulfide nanopore," *Nanoscale*, vol. 10, no. 41, pp. 19450–19458, 2018.

[66] S. Peng, Z. Yang, X. Ni, H. Zhang, J. Ouyang, and O. Fangping, "DNA translocation through graphene nanopores: a first-principles study," *Mater. Res. Express*, vol. 1, no. 1, p. 015044, 2014.

[67] J. Prasongkit *et al.*, "Topological line defects around graphene nanopores for DNA sequencing," *J. Phys. Chem. C*, vol. 122, no. 13, pp. 7094–7099, 2018.

[68] H. Qiu, A. Sarathy, J.-P. Leburton, and K. Schulten, "Intrinsic stepwise translocation of stretched ssDNA in graphene nanopores," *Nano Lett.*, vol. 15, no. 12, pp. 8322–8330, 2015.

[69] J. B. Heng *et al.*, "Stretching DNA using the electric field in a synthetic nanopore," *Nano Lett.*, vol. 5, no. 10, pp. 1883–1888, 2005.

[70] H. Qiu, A. Girdhar, K. Schulten, and J.-P. Leburton, "Electrically tunable quenching of DNA fluctuations in biased solid-state nanopores," *ACS Nano*, vol. 10, no. 4, pp. 4482–4488, 2016.

[71] D. J. Niedzwiecki, B. DiPaolo, C.-Y. Lin, A. Castan, R. Keneipp, and M. Drndic, "Devices for Nanoscale Guiding of DNA through a 2D Nanopore," *ACS Sens.*, vol. 6, no. 7, pp. 2534–2545, 2021.

[72] A. Storm, J. Chen, X. Ling, H. Zandbergen, and C. Dekker, "Fabrication of solid-state nanopores with single-nanometre precision," *Nat. Mater.*, vol. 2, no. 8, pp. 537–540, 2003.

[73] A. T. Kuan, B. Lu, P. Xie, T. Szalay, and J. A. Golovchenko, "Electrical pulse fabrication of graphene nanopores in electrolyte solution," *Appl. Phys. Lett.*, vol. 106, no. 20, 2015.

[74] J. Feng *et al.*, "Electrochemical reaction in single layer MoS2: nanopores opened atom by atom," *Nano Lett.*, vol. 15, no. 5, pp. 3431–3438, 2015.

[75] M. Thakur *et al.*, "Wafer-Scale Fabrication of Nanopore Devices for Single-Molecule DNA Biosensing using MoS2," *Small Methods*, vol. 4, no. 11, p. 2000072, 2020.

[76] Huber, S. et al. "Oxygen-stabilized triangular defects in hexagonal boron nitride." *Phys. Rev. B* 92, 245310 (2015).

[77] H. Qiu, A. Sarathy, K. Schulten, and J.-P. Leburton, "Detection and mapping of DNA methylation with 2D material nanopores," *Npj 2D Mater. Appl.*, vol. 1, no. 1, p. 3, 2017.

[78] J. Wilson, L. Sloman, Z. He, and A. Aksimentiev, "Graphene nanopores for protein sequencing," *Biophys. J.*, vol. 110, no. 3, p. 326a, 2016.

[79] J. Schreiber *et al.*, "Error rates for nanopore discrimination among cytosine, methylcytosine, and hydroxymethylcytosine along individual DNA strands," *Proc. Natl. Acad. Sci.*, vol. 110, no. 47, pp. 18910–18915, 2013.

[80] Á. Díaz Carral, M. Ostertag, and M. Fyta, "Deep learning for nanopore ionic current blockades," *J. Chem. Phys.*, vol. 154, no. 4, 2021.

[81] X.-L. Xing *et al.*, "Nanopores in 2D materials and their applications in single molecule analysis," *TrAC Trends Anal. Chem.*, vol. 179, p. 117863, 2024.